Article

Structural Mimicry of Retroviral Tat Proteins by Constrained β-Hairpin Peptidomimetics: Ligands with High Affinity and Selectivity for Viral TAR RNA Regulatory Elements

Zafiria Athanassiou, Ricardo L. A. Dias, Kerstin Moehle, Neil Dobson, Gabriele Varani, and John A. Robinson

J. Am. Chem. Soc., **2004**, 126 (22), 6906-6913• DOI: 10.1021/ja0497680 • Publication Date (Web): 14 May 2004

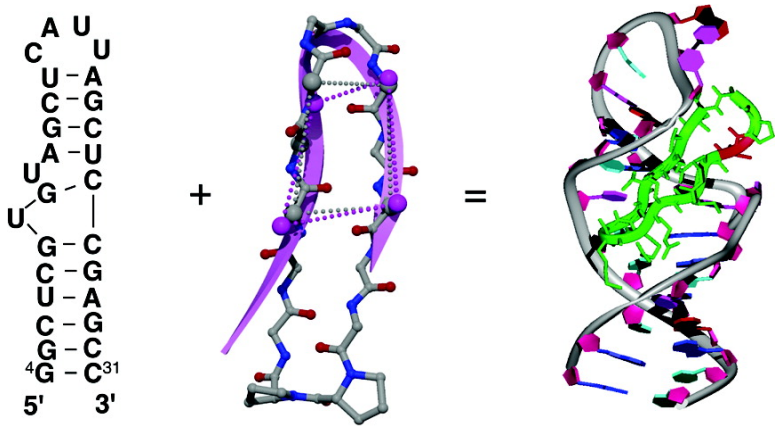

More About This Article

Additional resources and features associated with this article are available within the HTML version:

- Supporting Information
- Links to the 2 articles that cite this article, as of the time of this article download
- Access to high resolution figures
- Links to articles and content related to this article
- Copyright permission to reproduce figures and/or text from this article

View the Full Text HTML

J|A|C|S
ARTICLES
Published on Web 05/14/2004

Structural Mimicry of Retroviral Tat Proteins by Constrained β-Hairpin Peptidomimetics: Ligands with High Affinity and Selectivity for Viral TAR RNA Regulatory Elements

Zafiria Athanassiou,[†] Ricardo L. A. Dias,[†] Kerstin Moehle,[†] Neil Dobson,[‡] Gabriele Varani,*[,‡] and John A. Robinson*[,†]

Contribution from the Organic Chemistry Institute, University of Zürich, Winterthurerstrasse 190, 8057 Zürich, Switzerland, and Department of Chemistry and Department of Biochemistry, University of Washington, Seattle, Washington 98195

Received January 14, 2004; E-mail: robinson@oci.unizh.ch; varani@chem.washington.edu

Abstract: An approach is described to the design of β-hairpin peptidomimetic ligands for bovine immunodeficiency virus (BIV) Tat protein, which inhibit binding to its transactivator response element (TAR) RNA. A library of peptidomimetics was derived by grafting onto a hairpin-inducing D-Pro-L-Pro template sequences related to the RNA recognition element in Tat. One hairpin mimetic was identified that binds tightly ($K_d \approx 150$ nM) to BIV TAR, and another that binds also to HIV-1 TAR RNA ($K_d \approx 1-2$ μM). (In the same assay, the wild-type BIV Tat(65−81) peptide binds to BIV TAR with $K_d \approx 50$ nM.) The high-affinity BIV-Tat mimetic was shown to adopt a stable β-hairpin conformation in free solution by NMR methods. Amino acid substitutions in this mimetic were shown to impact on the hairpin structure and to disrupt binding to the RNA. This family of conformationally constrained peptidomimetics affords insights into the structural requirements for binding to TAR RNA and provides a basis for the design of new ligands with increased inhibitory activity and specificity to both BIV and HIV TAR RNAs.

Introduction

RNA−protein regulatory elements, such as the Tat−TAR and rev−RRE interactions of HIV and related immunodeficiency viruses,[1−3] are attractive targets for the discovery of new antiviral drugs.[4−7] The transcriptional activator proteins (Tat) play critical roles in the viral life cycle and contribute significantly to pathogenesis by increasing transcription of the integrated pro-virus.[8,9] In contrast to other viral transcriptional activators, Tat proteins do not recognize DNA promoter elements nor do they affect significantly transcriptional initiation. Rather, they recognize specific viral RNA elements called transactivator response elements (TAR) at the 5′-end of RNA transcripts. Upon formation of the Tat−TAR complex, a cellular cyclin/cyclin-dependent kinase complex (cyclin T1 − Cdk9) is recruited that positively regulates transcriptional elongation by enhancing phosphorylation of the C-terminal repeat of the large subunit of RNA polymerase II.[10]

The Tat−TAR interaction is essential for viral replication. Single nucleotide or amino acid substitutions within either the protein or the RNA severely affect transcriptional levels and hence viral replication.[1] This strong dependence of Tat−TAR function on sequence makes inhibition of the interaction an attractive target for antiviral therapy,[11−14] because resistance may be slow or difficult to develop.

RNA−protein complexes such as Tat−TAR have proven difficult targets for conventional small molecule inhibitor design. This may be due to the large surface interfaces buried in the complexes, as well as the inherent flexibility of both RNA and protein in the free states, which seem to favor mutually induced fit mechanisms of binding.[15] Earlier attempts to inhibit the Tat−TAR interaction using linear peptides,[16,17] or analogues such as peptoids,[18] provided limited structure/activity relationships, because of the inherent flexibility of these molecules in solution

[†] University of Zurich.
[‡] University of Washington.

(1) Fischer, U.; Huber, J.; Boelens, W. C.; Mattaj, I. W.; Lührmann, R. *Cell* **1995**, *82*, 475−483.
(2) Graeble, M. A.; Churcher, M. J.; Lowe, A. D.; Gait, M. J.; Karn, J. *Proc. Natl. Acad. Sci. U.S.A.* **1993**, *90*, 6184−6188.
(3) Dingwall, C.; Ernberg, I.; Gait, M. J.; Green, S. M.; Heaphy, S.; Karn, J.; Lowe, A. D.; Singh, M.; Skinner, M. A.; Valerio, R. *Proc. Natl. Acad. Sci. U.S.A.* **1989**, *86*, 6925−6929.
(4) Gallego, J.; Varani, G. *Acc. Chem. Res.* **2001**, *34*, 836−843.
(5) Wilson, W. D.; Li, K. *Curr. Med. Chem.* **2000**, *7*, 73−98.
(6) Kirk, S. R.; Luedtke, N. W.; Tor, Y. *J. Am. Chem. Soc.* **2000**, *122*, 980−981.
(7) Mei, H.-Y.; Cui, M.; Heldsinger, A.; Lemrow, S. M.; Loo, J. A.; Sannes-Lowery, K. A.; Sharmeen, L.; Czarnik, A. W. *Biochemistry* **1998**, *37*, 14204−14212.
(8) Gonda, M. A.; Luther, D. G.; Fong, S. E.; Tobin, G. J. *Virus Res.* **1994**, *32*, 155−181.
(9) Jones, K. A.; Peterlin, B. M. *Annu. Rev. Biochem.* **1994**, *63*, 717−743.
(10) Wei, P.; Garber, M. E.; Fang, S.-M.; Fischer, W. H.; Jones, K. A. *Cell* **1998**, *92*, 451−462.
(11) Tok, J. B.-H.; Des Jean, R. C.; Fenker, J. *Bioorg. Med. Chem. Lett.* **2001**, *11*, 43−46.
(12) Smith, C. *Mol. Cell* **2000**, *6*, 1067−1076.
(13) Frankel, A. D. *Curr. Opin. Struct. Biol.* **2000**, *10*, 332−340.
(14) Xavier, K. A.; Eder, P. S.; Giordano, T. *Trends Biotechnol.* **2000**, *18*, 349−356.
(15) Leulliot, N.; Varani, G. *Biochemistry* **2001**, *40*, 7947−7956.
(16) Huq, I.; Wang, X.; Rana, T. M. *Nat. Struct. Biol.* **1997**, *4*, 881−882.
(17) Huq, I.; Ping, Y.-H.; Tamilarasu, N.; Rana, T. M. *Biochemistry* **1999**, *38*, 5172−5177.
(18) Hamy, F.; Felder, E. R.; Heizmann, G.; Lazdins, J.; Aboul-ela, F.; Varani, G.; Karn, J.; Klimkait, T. *Proc. Natl. Acad. Sci. U.S.A.* **1997**, *94*, 3548−3553.

10.1021/ja0497680 CCC: $27.50

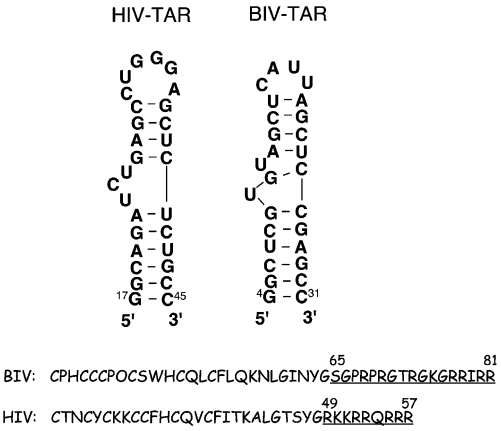

Figure 1. Secondary structures of HIV-1 and BIV TAR RNA, and partial sequences of HIV-1 and BIV Tat proteins with the arginine-rich RNA-binding domains underlined.

and a lack of knowledge of their bound structures. Here, we sought to identify conformationally restrained peptidomimetic Tat inhibitors and to develop structure−activity relationships for use in inhibitor optimization.

Structural information is not yet available on the HIV Tat−TAR complex, although large and well-characterized changes in conformation of HIV TAR occur when peptides derived from Tat, or even the single amino acid derivative argininamide, bind to it.[19−23] The function of Tat and TAR is conserved among lentiviruses, including bovine immunodeficiency virus (BIV). The sequences of BIV and HIV-1 TAR are highly similar (Figure 1). Moreover, the 3D structure of BIV TAR in a complex with a Tat-derived peptide has been solved by multidimensional heteronuclear NMR methods (Figure 2).[24,25] These studies revealed a well-defined β-hairpin conformation in the bound Tat peptide. This makes the BIV TAR−Tat system an attractive model for inhibitor design, based on conformationally restrained β-hairpin peptidomimetics.

The design of RNA-binding molecules has been reviewed extensively.[4,26−28] Well-known RNA ligands include the aminoglycoside (and other) antibiotics, heterocycles, intercalators and polycations, as well as various linear peptides and peptoids. As this work was being prepared for publication, the first example of a backbone cyclic peptide that targets BIV TAR RNA was reported.[29] In this work, we show that conformationally restrained peptidomimetics having well-defined folded structures offer the prospect of developing structure−activity relationships that may be useful in design and optimizing ligand affinity to RNA. We describe a family of cyclic β-hairpin peptidomimetics of BIV Tat, together with binding studies, which demonstrate their specific inhibition of the Tat/TAR interaction of both BIV and HIV. We also show that these TAR−Tat peptidomimetics fold into stable β-hairpin conformations in free solution and that formation of this structure favors binding, thus validating the design principle.

Experimental Section

Peptide Synthesis. Abbreviations: Boc, *tert*-butoxycarbonyl; DMF, *N*,*N*-dimethylformamide; Fmoc, 9-fluorenylmethoxycarbonyl; HATU, 2-(1*H*-9-azabenzotriazole-1-yl)-1,1,3,3-tetramethyluronium hexafluorophosphate; HBTU, 2-[1*H*-benzotriazole-1-yl]-1,1,3,3-tetramethyluronium hexafluorophosphate; HOAt, *N*-hydroxy-9-azabenzotriazole; HOBt, *N*-hydroxybenzotriazole; Pbf, 2,2,4,6,7-pentamethyldihydrobenzofuran-5-sulfonyl; TIPS, triisopropylsilane; TFA, trifluoroacetic acid.

Peptides were synthesized by solid-phase peptide synthesis using standard Fmoc-chemistry.[30,31] Resin and protected amino acids were from *Novabiochem* (Switzerland). After purification, all peptides were analyzed by MS, NMR, and amino acid analysis. The concentration of each peptide was determined by UV absorbance (280 nm, for peptides containing Tyr) or by quantitative amino acid analysis.

The wild-type BIV Tat-derived peptide (residues 65−81, Ac−SGPRPRGTRGKGRRIRR−NH_2) was prepared on MBHA-Rink amide resin using Fmoc-chemistry on an Applied Biosystems 433A peptide synthesizer. Acetylation of the N-terminus was performed with acetic

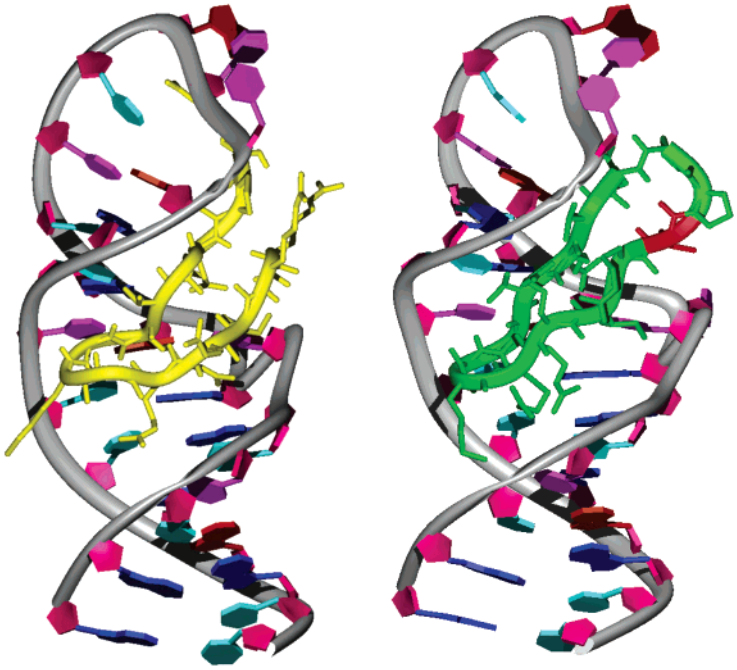

Figure 2. Left: The BIV Tat peptide (yellow) adopts a β-hairpin conformation upon binding to the TAR RNA[24,25] (prepared using PDB file 1MNB). Right: A model of the BIV2−TAR complex (green with Val^2 in red), with BIV2 bound in the major groove of BIV TAR RNA. The model was generated by replacing the BIV Tat peptide in the structure of the BIV Tat−TAR complex (left) with one of the structures of the BIV2 peptide calculated as described in the text. No further modification of the model was performed.

Table 1. Sequences of β-Hairpin Mimetics BIV1−BIV8, and Summary of K_d Values (in μM) Determined for the Interaction of Each Mimetic with BIV TAR RNA (nd = no binding detected)[a]

Mimetic	Position												K_d
	1	*2*	*3*	*4*	*5*	*6*	*7*	*8*	*9*	*10*	*11*	*12*	
BIV1	I	R	G	T	R	G	K	R	R	I	R	V	30
BIV2	R	V	R	T	R	G	K	R	R	I	R	V	0.15
BIV3	I	Y	R	T	R	G	K	R	R	I	R	T	nd
BIV4	Y	R	G	T	R	G	K	R	R	I	Y	V	>50
BIV5	R	R	G	T	R	G	K	R	R	I	G	R	1-2
BIV6	V	R	G	T	R	G	K	R	R	I	K	Y	>50
BIV7	V	R	R	T	R	G	K	R	R	I	K	Y	nd
BIV8	K	R	G	T	R	G	K	R	R	I	G	Y	>50

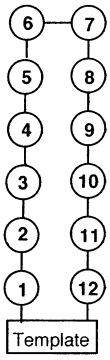

[a] A representation of a typical 12-residue loop in a 2:2 β-hairpin conformation mounted on the D-Pro-L-Pro template is shown on the right. The residues at positions 4−10 remain constant (see text).

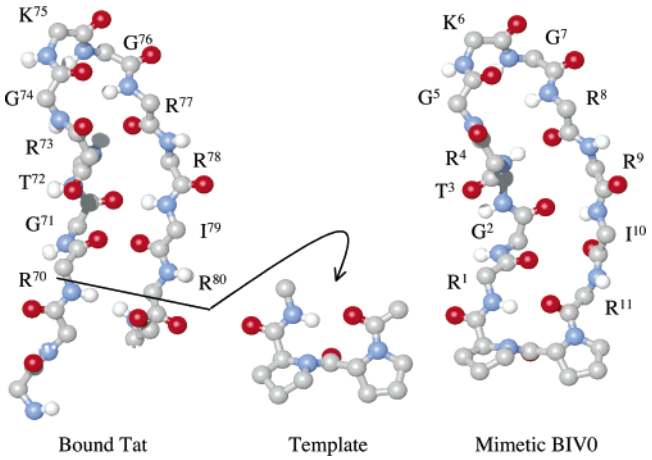

Figure 3. The design of mimetic BIV0 is illustrated. The conformation of Tat bound to TAR (left), the D-Pro-L-Pro template (middle), and a model of BIV0 (right) are shown. O atoms are in red; N atoms are in blue.

anhydride and pyridine. The product was purified by reverse phase HPLC (Vydac, C_4 column, gradient from 5% to 80% MeCN in H_2O + 0.1% TFA).

For BIV0 (*cyclo*-(−Gly−Arg−Thr−Gly−Arg−Pro−DPro−Arg−Ile−Arg−Arg−Gly−Lys−)), Fmoc−Gly−OH (0.6 mmol, 178.4 mg) (residue 5, Figure 3) was coupled first to 2-chlorotrityl chloride resin (0.6 g, 1.2 mmol/g), and linear peptide assembly was performed using standard Fmoc-chemistry (20% piperidine in DMF for Fmoc deprotection, HOBt/HBTU for activation (4 equiv), diisopropylethylamine as base, and *N*-methylpyrrolidone as solvent). After completion of the synthesis, the linear precursor was cleaved from the resin using 0.5% TFA in CH_2Cl_2. Cyclization was performed in DMF solution (5 mg/mL) with HATU, HOAt (3 equiv), and diisopropylethylamine. The protected cyclic peptide was treated with TFA/TIPS/H_2O (95/2.5/2.5) at room temperature for 4 h. After precipitation by diethyl ether, BIV0 was purified by reverse phase HPLC (Vydac, C_{18} column, gradient from 5% to 100% MeCN in H_2O + 0.1% TFA).

Peptides BIV1−BIV8 were synthesized in parallel on a MultiSynTech-Syro peptide synthesizer. Fmoc−Gly−OH (0.6 mmol) (residue 6, Table 1) was coupled to 2-chlorotrityl chloride resin (0.6 g, 1.2 mmol/g). Chain elongations were performed with HBTU/HOBt (4 equiv) as coupling reagents and diisopropylethylamine as base. Each coupling step was carried out twice to ensure complete coupling. Upon completion of the assembly, the linear side-chain-protected peptides were cleaved from the resin with 0.5% TFA in CH_2Cl_2. Each crude linear peptide was then cyclized in DMF solution with HATU/HOAt as coupling reagents and diisopropylethylamine as base. After DMF removal, the cyclic protected peptides were treated with TFA/TIPS/H_2O (95/2.5/2.5) at room temperature for 4 h. Precipitation with diethyl ether and purification by reverse phase HPLC (Vydac, C_{18} column, gradient from 5% to 100% MeCN in H_2O + 0.1% TFA) gave mimetics BIV1−BIV8. Each mimetic showed one peak (>98%) with the correct mass when analyzed by HPLC-MS.

RNA Preparation and Gel Shift Assays. Labeled RNA was prepared by in vitro transcription using T7 RNA polymerase, a synthetic oligonucleotide template, and a nucleotide mixture containing [α-^{32}P]-CTP (3000 Ci/mmol).[32] The RNA oligonucleotides were purified by denaturing PAGE, and concentrations were determined by UV at 260 nm. RNA was annealed by heating at 90 °C and slow cooling to room temperature in sterile H_2O at a concentration of 20−100 nM. Binding assays were performed at 4 °C. Peptide and RNA were incubated in buffer (10 μL) containing Tris-HCl (50 mM, pH 8.0), KCl (50 mM), DTT (200 mM), tRNA (*E. coli*, 280 μg/mL), and Triton X-100 (0.05%). The samples were fractionated by loading into 12% native polyacrylamide gels in 0.5% TB buffer and electrophoresed at 15 W and 4 °C. Dried gels were exposed to a phosphor imaging plate and scanned with a Molecular Dynamics phosphor imager. Bands corresponding to free and bound RNA were quantified using ImageQuant software.

NMR Spectroscopy. 1D and 2D NMR spectra of peptides were recorded at 600 MHz (Bruker DRX-600 spectrometer) or 500 MHz (Bruker AMX-500 spectrometer) typically at a peptide concentration of 10−20 mg/mL in H_2O/D_2O 9:1 at pH 5.0 or 2.3. Water suppression was performed by presaturation. Spectral assignments were based on DQF-COSY and TOCSY spectra. Distance restraints were obtained from NOESY and/or ROESY spectra. Spectra were typically collected with 512 real (TPPI) or 256 complex (States-TPPI) points in the indirect dimension. For NOESY, ROESY, and off-resonance ROESY spectra, a cosine window function was applied in both dimensions after zero-filling to 2k × 1k real points prior to Fourier transformation. Data processing was carried out with XWINNMR (Bruker) and Xeasy.[33]

(19) Puglisi, J. D.; Tan, R.; Canlan, B. J.; Frankel, A. D.; Williamson, J. R. *Science* **1992**, *257*, 76−80.
(20) Tan, R.; Frankel, A. D. *Biochemistry* **1992**, *31*, 10288−10294.
(21) Aboul-ela, F.; Karn, J.; Varani, G. *J. Mol. Biol.* **1995**, *253*, 313−332.
(22) Aboul-ela, F.; Karn, J.; Varani, G. *Nucleic Acids Res.* **1996**, *24*, 3974−3981.
(23) Al-Hashimi, H. M.; Gosser, Y.; Gorin, A.; Hu, W.; Majumdar, A.; Patel, D. J. *J. Mol. Biol.* **2002**, *315*, 95−102.
(24) Ye, X.; Kumar, R. A.; Patel, D. J. *Chem. Biol.* **1995**, *2*, 827−840.
(25) Puglisi, J. D.; Chen, L.; Blanchard, S.; Frankel, A. D. *Science* **1995**, *270*, 1200−1203.
(26) Herrmann, T. *Angew. Chem., Int. Ed.* **2000**, *39*, 1890−1904.
(27) Sucheck, S. J.; Wong, C.-H. *Curr. Opin. Chem. Biol.* **2000**, *4*, 678−686.
(28) Cheng, A.; Calabro, V.; Frankel, A. *Curr. Opin. Struct. Biol.* **2001**, *11*, 478−484.
(29) Runyon, S. T.; Puglisi, J. D. *J. Am. Chem. Soc.* **2003**, *125*, 15704−15705.
(30) Atherton, E.; Sheppard, R. C. *Solid-phase Peptide Synthesis-A Practical Approach*; IRL Press: Oxford, 1989.
(31) Fields, G. B.; Noble, R. L. *Int. J. Pept. Protein Res.* **1990**, *35*, 161−214.
(32) Milligan, J. *Nucleic Acids Res.* **1987**, *15*, 8733−8798.

NMR spectra of the free RNA and RNA−peptide complexes were recorded at 750 MHz (Bruker DMX-750) at RNA concentrations of 0.5−1.0 mM either in D_2O or in H_2O/D_2O (20:1) at pH 6.2−6.6 in phosphate buffer. The complexes were formed at 1:1 equimolar ratio by titration of the RNA with increasing amounts of peptide. Formation of the complex was monitored by TOSCY spectra. Water suppression was performed with Watergate.[34] Data processing and analysis was carried out with XWINNMR (Bruker) and Sparky 3.106 (UCSF, USA).

Structural Calculations. Structure calculations were performed by restrained molecular dynamics in torsion angle space by applying the simulated annealing protocol implemented in DYANA.[35] Restrained energy minimization was performed with GROMOS.[36] MOLMOL[37] and GRASP[38] were used for structure analysis and visualization of molecular models.

Results

Design of the Library. The starting point for the design of BIV0 was the structure of Tat (residues 70-RGTRGKGRRIR-80) bound to TAR (PDB file 1MNB),[25] together with mutagenesis data showing[39] that residues in Tat critical for TAR binding include Arg^{70}, Gly^{71}, Thr^{72}, Arg^{73}, Gly^{74}, Arg^{77}, and Ile^{79}, which are all located close to the reverse turn formed by residues Gly^{74}, Lys^{75}, and Gly^{76}. Transplanting the residues 70−80 from Tat onto the D-Pro-L-Pro template gives the mimetic BIV0 (see Figure 3).

In principle, a regular 2:2 β-hairpin conformation[40] will be preferred by a 12-residue loop (BIV0 contains 11 residues) mounted on the D-Pro-L-Pro template.[41,42] A small eight-member library (Table 1) of hairpin mimetics (BIV1−BIV8) was, therefore, designed containing 12 amino acids loops. Residues Thr^4, Arg^5, Gly^6, Lys^7, Arg^8, Arg^9, and Ile^{10} were held constant because corresponding residues in Tat (Thr^{72}−Ile^{79}) are important for binding to TAR. The remaining positions were filled with cationic or aliphatic/aromatic residues, on the basis of visual inspection of computer models. The sequences of the resulting library members are shown in Table 1.

Peptide Synthesis. The 17-residue wild-type Tat-derived control peptide Ac−^{65}SGPRPRGTRGKGRRIRR^{81}−NH_2 (BIV Tat(65−81)) was produced by solid-phase peptide synthesis following standard Fmoc-chemistry. The BIV mimetics were synthesized by first assembling a linear peptide chain on 2-chlorotrityl chloride resin. The linear precursor was then cleaved from the resin, without removing side-chain protecting groups, and macrocyclization was performed in dilute DMF solution. The side-chain protecting groups were then removed with trifluoroacetic acid, and the products were purified by reverse phase HPLC. In a typical synthesis, the main component in the crude product was the desired BIV mimetic, which after purification was obtained in 15−25% overall yield.

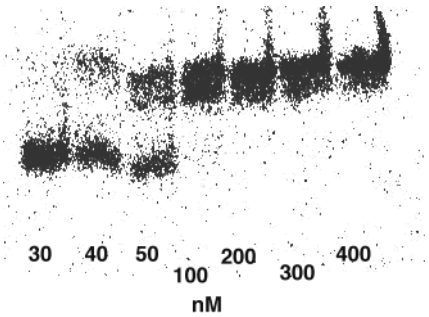

Figure 4. Gel band shift assays of Tat-derived wt peptide (BIV65-81) with BIV TAR RNA (at 2 nM concentration). Peptide concentrations are shown.

Binding Assays with TAR RNA. The wild-type peptide BIV Tat(65−81) was used as a positive control in all binding studies. The dissociation constant (K_d) of this peptide determined by polyacrylamide gel band shift assays in Tris-HCl buffer (50 mM, pH 8.0, KCl (50 mM)) was 50 nM (Figure 4). This value is approximately 10-fold higher than that reported,[43] perhaps due to differences in the assay conditions (higher tRNA concentrations, absence of glycerol in the gels, and different ionic strength buffers). Moreover, binding of the wild-type peptide to TAR RNA did not give rise to a single shifted band, corresponding to the Tat−TAR complex; rather this shifted band appeared as two very closely spaced bands, only the upper one of which was present at saturating peptide concentrations (>500 nM). Only a single shifted band corresponding to the ligand-bound form of TAR RNA was seen in each of the assays with the BIV peptidomimetics (see Figure 5). However, upon binding of BIV0 to BIV TAR RNA, the band shift upon complex formation was too small to allow accurate quantitation of binding (data not shown). We therefore used an inhibition assay, where the BIV0 peptidomimetic was added to a preformed complex of BIV Tat(65−81) and TAR RNA, and the displacement of the peptide in the complex by BIV0 was monitored. This revealed an IC_{50} of ∼40 μM (data not shown).

Binding of the 12-residue loop mimetics (BIV1−BIV8) to BIV TAR RNA was also monitored by band shift assays (for K_d values, see Table 1). This gave a K_d of ∼30 μM for BIV1 binding to TAR RNA, while a $K_d \approx 150$ nM was found for BIV2 (Figure 5). The RNA-binding activity of BIV2 was highly specific, because no binding of BIV2 could be detected with HIV-1 TAR RNA (data not shown).

Under the same conditions, BIV3 showed no binding activity toward BIV TAR, and BIV4 exhibits only very weak binding (data not shown). In contrast, BIV5 was found to bind both BIV and HIV-1 TAR RNA with a K_d of 1−2 μM (Figure 5). BIV5 is the only mimetic tested which exhibits affinity for both BIV and HIV TAR RNA. BIV6 and BIV8 were also found to be poorly bound even at high micromolar concentrations (data not shown), while the band shift assays for BIV7 failed because, in the presence of TAR RNA, the sample repeatedly precipitated rather than entering the polyacrylamide gel.

Conformational Studies. The structures of peptidomimetics BIV0−BIV8 were investigated in aqueous solution by ^{1}H NMR spectroscopy. The 1D and 2D ^{1}H NMR spectra of BIV0 revealed two main forms in solution in a ∼2:1 ratio that interchange

(33) Bartels, C.; Xia, T.; Billeter, M.; Guentert, P.; Wüthrich, K. *J. Biomol. NMR* **1995**, *6*, 1−10.
(34) Lippens, G.; Dhallium, C.; Wieruszeski, J. M. *J. Biomol. NMR* **1995**, *5*, 327−331.
(35) Guntert, P.; Mumenthaler, C.; Wüthrich, K. *J. Mol. Biol.* **1997**, *273*, 283−298.
(36) Van Gunsteren, W. F.; Billeter, S. R.; Eising, A. A.; Hünenberger, P. H.; Krüger, P.; Mark, A. E.; Scott, W. R. P.; Tironi, I. G. *Biomolecular Simulation: The GROMOS96 Manual and User Guide*; Hochschulverlag AG an der ETH Zurich, 1996.
(37) Koradi, R.; Billeter, M.; Wüthrich, K. *J. Mol. Graphics* **1996**, *14*, 51−55.
(38) Nicholls, A.; Sharp, K. A.; Honig, B. *Proteins* **1991**, *11*, 281−296.
(39) Chen, L.; Frankel, A. D. *Proc. Natl. Acad. Sci. U.S.A.* **1995**, *92*, 5077−5081.
(40) Sibanda, B. L.; Blundell, T. L.; Thornton, J. M. *J. Mol. Biol.* **1989**, *206*, 759−777.
(41) Favre, M.; Moehle, K.; Jiang, L.; Pfeiffer, B.; Robinson, J. A. *J. Am. Chem. Soc.* **1999**, *121*, 2679−2685.
(42) Jiang, L.; Moehle, K.; Dhanapal, B.; Obrecht, D.; Robinson, J. A. *Helv. Chim. Acta* **2000**, *83*, 3097−3112.
(43) Chen, L.; Frankel, A. D. *Biochemistry* **1994**, *33*, 2708−2715.

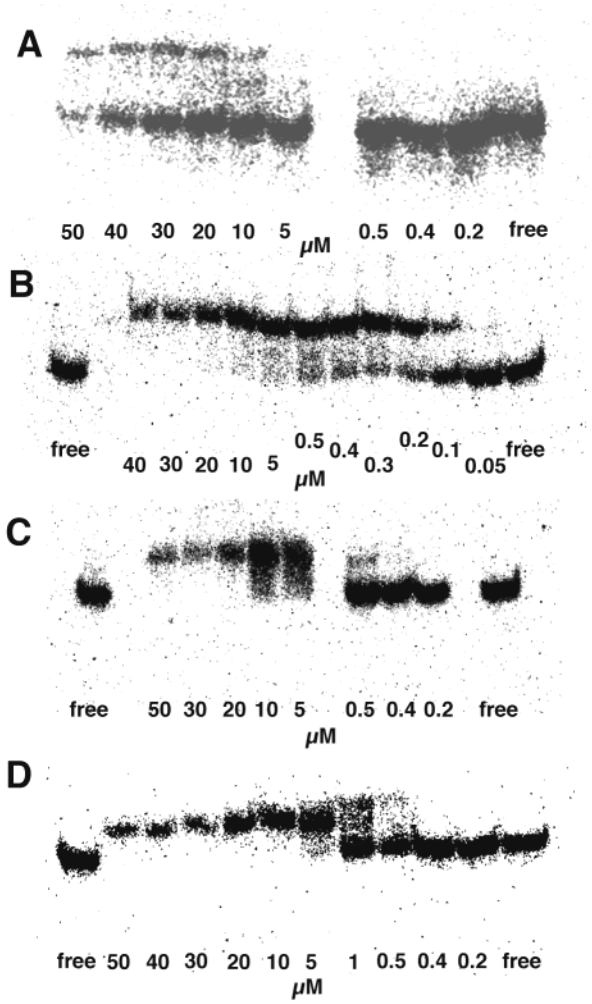

Figure 5. (A) Binding of BIV1 to BIV TAR (9 nM). (B) Binding of BIV2 to BIV TAR (9 nM). (C) Binding of BIV-5 to BIV TAR (9 nM). (D) Binding of BIV-5 to HIV-1 TAR RNA (2 nM). Peptide concentrations are also shown.

slowly on the NMR time scale, as well as additional minor species (<10%) that were not investigated further. Due to overlap, it was not possible to fully assign the ^{1}H spectrum. The two major forms appear to be trans−cis (2:1) isomers at the Arg^{11}-D-Pro^{12} peptide bond, because an Arg^{11} C(α)−H to D-Pro^{12} C(α)−H NOE, characteristic of a cis peptide bond, could be assigned in the minor form. Using the other available assignments, only a few cross-strand NOEs expected for a regular β-hairpin structure were found (Figure 6A).

The ^{1}H NMR spectra of BIV1 also showed two forms in solution, in a 9:1 ratio, clearly recognizable as trans−cis (9:1) isomers at the Val^{12}−D-Pro^{13} peptide bond. Only one significant NH−NH NOE was observed, between the peptide NHs of Lys^7 and Arg^8. In contrast, BIV2 appeared as a single species (>95%) in solution, with a strong Val^{12} C(α)−H to D-Pro^{13} C(δ)−H NOE in NOESY spectra typical for a trans peptide bond. Many NH−NH NOE connectivities were seen, including as the strongest that between the Lys^7 and Arg^8 peptide NHs (Figure 6B). Many other cross-strand NOE connectivities provided compelling prima facia evidence for a stable β-hairpin structure. Similar results were found for BIV3, which also comprised a single major species in solution, with all peptide bonds trans, and many peptide NH−NH and other cross-strand NOE connectivities observable in NOESY spectra. That many of the

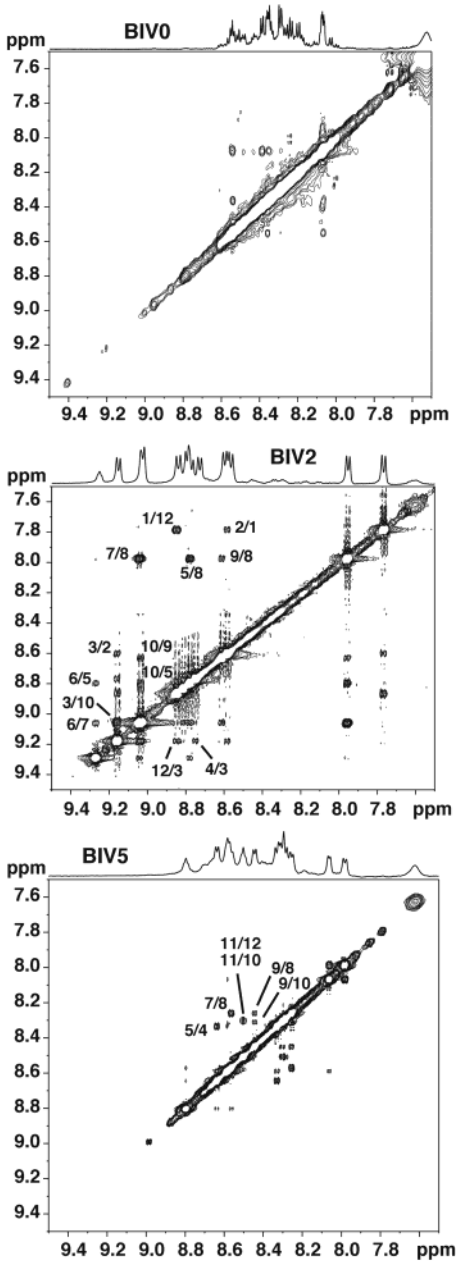

Figure 6. NH−NH NOEs in 2D NOESY or ROESY spectra for (top) BIV0 (ROESY, full assignment not available); (middle) BIV2 (NOESY, assignments shown); and (bottom) BIV5 (NOESY, with assignments).

$^3J_{HN-H\alpha}$ coupling constants are >9.0 Hz for residues in BIV2 and BIV3 flanking the expected turn region (Gly^6−Lys^7) is a further indication of a stable β-hairpin structure in both peptides.[44]

Whereas BIV4 and BIV7 each showed a single set of ^{1}H NMR signals, consistent with one main species in solution, spectra of BIV6 and BIV8 each showed about 5−10% of a minor form. The single forms of BIV4 and BIV7 and the major forms of BIV6 and BIV8 all showed NOEs consistent with a trans peptide bond preceding D-Pro^{13}. The ^{1}H NMR spectra of BIV5 revealed a more complicated picture, with one main and two minor species in an approximately 8:1:1 ratio. Due to problems of overlap, only the spectrum of the major form of

(44) Wüthrich, K. *NMR of Proteins and Nucleic Acids*; John Wiley & Sons: New York, 1986.

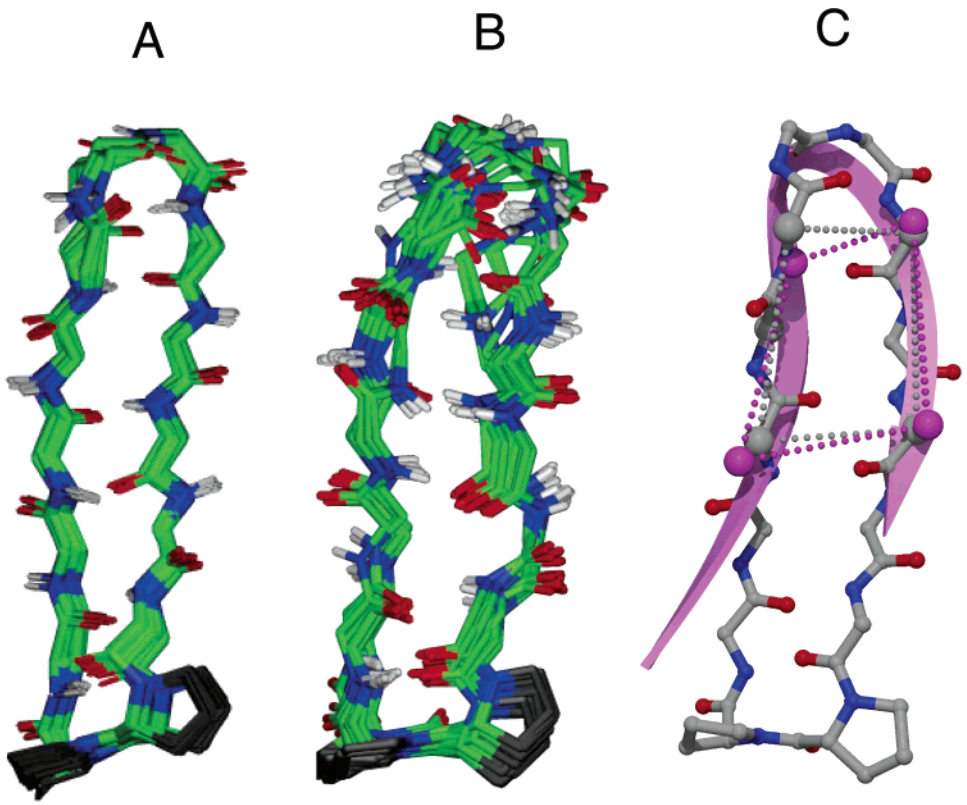

Figure 7. (A) Superposition of the final 20 NMR structures for BIV2. (B) Superposition of the final 20 NMR structures for BIV3; each in aqueous solution at pH 2.3. (C) Superposition of the C(α) positions of residues Arg^{2}, Thr^{4}, Arg^{5}, Arg^{8}, and Ile^{10} (grey) in a typical NMR structure of BIV2 with the corresponding C(α) positions (of residues Arg^{70}, Thr^{72}, Arg^{73}, Arg^{77}, and Ile^{79}) (magenta) in the bound form of wt BIV Tat peptide[25] (from 1MNB). See also Figure 2.

Table 2. Experimental Restraints and Statistics for the Final 20 NMR Structures Calculated for BIV2 and BIV3

	Biv2	Biv3
NOE upper-distance restraints	131	111
intraresidue	47	39
sequential	63	44
medium- and long-range	21	28
residual target function value (Å^2)	0.81 ± 0.12	0.52 ± 0.04
mean rmsd values (Å)		
all backbone atoms	0.42 ± 0.18	1.04 ± 0.48
all heavy atoms	1.84 ± 0.26	2.64 ± 0.75
residual NOE violation		
number > 0.2 Å	25	0
maximum (Å)	0.31	0.18

BIV5 could be assigned. For the single forms of BIV4 and BIV7 as well as the major forms of BIV5, BIV6, and BIV8, the $^3J_{HN-H\alpha}$ coupling constants of each were all in the range typical for fast conformational averaging (6−8 Hz), and only a few medium- and long-range NOEs typical of a regular β-hairpin could be detected in NOESY spectra (Figure 6C).

The aforementioned NMR data indicated that BIV2 and BIV3 adopt regular hairpin structures, while the other mimetics appear to adopt more diverse, multiple conformations. Structure calculations are, therefore, only reported for BIV2 and BIV3. For each peptide, the NOEs assigned in NOESY spectra were used to derive upper-distance restraints for structure calculations. The upper-distance restraints are provided in the Supporting Information. The set of structures calculated for each peptide were inspected for their relatedness to each other, and for consistency with the measured $^3J_{HN-H\alpha}$ coupling constants.

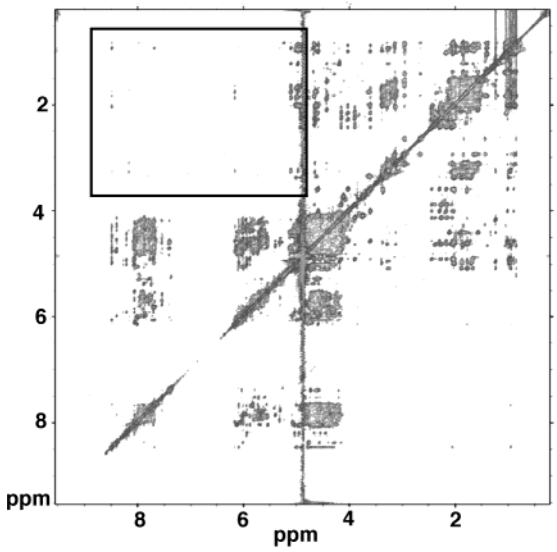

Figure 8. NOESY spectrum of the BIV2−TAR RNA complex in water (H_2O:D_2O, 9:1). The region of the spectrum containing intermolecular NOEs is boxed.

Although it is impossible here to describe fully the dynamics of these mimetics, the structure calculations provide to a first approximation a good description of the preferred average folded structures in solution.

The results of DYANA calculations for BIV2 and BIV3 are shown in Table 2 and Figure 7. The ensemble of 20 energy-minimized structures obtained for each mimetic converge to a family of closely related β-hairpin conformations, with minimal restraint violations, and predicted $^3J_{HN-H\alpha}$ coupling constants close to the values observed. The numerous long-range cross-

strand NOE restraints used in the DYANA calculations (see Supporting Information) account for the well-ordered antiparallel β-strands in the final structures. Peptide NH- -OC cross-strand hydrogen bonds are observed between residues Arg^1-Val^{12} (Ile^1-Thr^{12}) Arg^3-Ile^{10} Arg^5-Arg^8, as expected for regular 2:2 hairpin conformations,[40] with predominantly type-II′ β-turn conformations at the tip of each hairpin.

NMR Studies of BIV2−TAR RNA Complex. The BIV2 and BIV5 peptide−RNA complexes were studied by ^{1}H NMR spectroscopy in aqueous solution. Considerable exchange broadening of signals of TAR RNA occurred upon titration with BIV5, consistent with a relatively weak binding interaction. In contrast, the bound form of BIV2 was in slow exchange with the free form, as evident from the occurrence of two sets of cross-peaks for substoichiometric concentrations of BIV2. The NOESY spectrum of the BIV2−TAR RNA complex (Figure 8) revealed many intermolecular NOEs between the RNA and the peptidomimetic. These include NOE connectivities from BIV2 to RNA base pairs predicted to lie in close proximity to each other. These data confirm that the mimetic binds to the expected site on the RNA.

Discussion

To date, the design of novel small molecule ligands for RNA has not been straightforward, due to a lack of detailed knowledge about RNA−ligand binding mechanisms. The availability of three-dimensional NMR structures for complexes of BIV TAR RNA bound to a fragment of the Tat protein provided the starting point for this work.[24,25] The aim was to establish an approach to the discovery of novel ligands for immunodeficiency virus TAR RNA, by using the known conformation of bound BIV−Tat to design and then test conformationally restrained β-hairpin peptidomimetics as TAR−Tat inhibitors. Having peptidomimetic ligands available, of defined conformation in both the free and the bound states, provides new opportunities for studying mechanisms of RNA recognition, and for developing structure−activity relationships useful in inhibitor optimization.

Our first attempt to prepare a hairpin peptidomimetic followed the simple expedient of transplanting residues 70−80 of Tat, including all of those known to be important for binding to TAR RNA, onto a hairpin-inducing D-Pro-L-Pro template[41,42,45−47] (Figure 3). The resulting mimetic (BIV0), however, was neither a good ligand for BIV TAR RNA ($IC_{50} \approx 40$ μM) nor did it adopt a stable regular β-hairpin conformation, as evident from ^{1}H NMR spectra in aqueous solution. For BIV0, bands corresponding to free and bound species were too closely spaced to allow a quantitative analysis. Although there may be several reasons for the poor structural mimicry, it is conceivable that all of the bond vectors in residues 70 and 80 of the Tat peptide bound to TAR are not maintained accurately upon transfer of the loop to the D-Pro-L-Pro template. This is illustrated in Figure 3. A large proportion of a cis peptide bound linking residue-80 (Tat numbering) to D-Pro is seen in BIV0 in solution, and in the major (trans) isomer a regular hairpin conformation was not significantly populated. It seems likely that the poor affinity of BIV0 to the RNA target is due to the poor structural mimicry by BIV0 of bound Tat. If so, the energetic penalties associated with the adoption of the structure required for binding could be even higher than for the linear peptide, which is unstructured in free solution.[24,25]

After considering additional factors that would stabilize a β-hairpin conformation, a small library of new mimetics (BIV1−BIV8, Table 1) was designed comprising 12 residues mounted onto the D-Pro-L-Pro template. Seven amino acids, taken from $Thr^{72}-Ile^{79}$ in BIV Tat, were retained at positions 4−10 in all 12-mer loop mimetics, and the remaining five positions were filled with residues that appeared from inspection of models to be appropriate for binding to TAR RNA. Although this provides tremendous scope for variation, only eight library members were made and studied. Clearly, this library explores only a very small part of the combinatorial diversity potentially achievable at these nonconserved positions.

From a structural viewpoint, the goal of producing peptidomimetics populating stable β-hairpin conformations was achieved with BIV2 and BIV3. Both appeared by NMR to populate regular 2:2 hairpin conformations in aqueous solution (Figure 7). The remaining members of the library, however, adopt a more diverse array of conformations. For several members, only a few rather weak NOEs typical of cross-strand NOE connectivities were seen, and using these as restraints in structure calculations did not afford convergence to only regular β-hairpin structures (data not given), as seen for BIV2 and BIV3. The rules governing β-hairpin stability in this family of mimetics are not yet sufficiently well refined to fully explain these sequence-dependent conformational effects.

Of special interest is the inhibitory activity of the BIV1−BIV8 mimetics. One library member (BIV2) stands out as a high-affinity ligand ($K_d \approx 150$ nM) specific for BIV TAR RNA (Figure 5). Remarkably, the affinities of BIV2 to HIV-1 TAR RNA, as well as to tRNA, are >10 000-fold lower, demonstrating that the interaction between BIV2 and BIV TAR is highly specific. This level of selectivity is rarely observed in studies of RNA-binding small molecules; generally promiscuous binding to a variety of RNAs is observed. Superimposition of the backbones of the average BIV2 NMR structure and the linear Tat-derived peptide bound to BIV TAR (PDB 1MNB) (Figure 7C) demonstrates that the two structures are very similar. Furthermore, computer modeling suggests that BIV2 will also fit snugly into the major groove of the BIV TAR RNA (Figure 2).

Recently, a BIV Tat peptide mimic comprising a backbone cyclic peptide was described[29] that interacts with BIV TAR and adopts a bound structure similar to that of the linear Tat peptide. However, the cyclic peptide was unfolded in the absence of RNA, and no evidence of specific binding to BIV TAR was reported. By successfully prestructuring the mimetic BIV2, we are able to strongly enhance affinity and reduce nonspecific binding, even to the closely related HIV-1 TAR RNA. While prestructuring of the mimetic into a hairpin conformation should favor binding, it is not sufficient. BIV3 was also found by NMR to adopt a stable β-hairpin structure, but it does not bind significantly to TAR RNA. Inspection of models (Figure 2) suggests that upon replacing Val^2 by Tyr^2, steric clashes involving the Tyr^2 side chain would prevent binding: in the

(45) Späth, J.; Stuart, F.; Jiang, L.; Robinson, J. A. *Helv. Chim. Acta* **1998**, *81*, 1726−1738.
(46) Shankaramma, S. C.; Athanassiou, Z.; Zerbe, O.; Moehle, K.; Mouton, C.; Bernardini, F.; Vrijbloed, J. W.; Obrecht, D.; Robinson, J. A. *ChemBioChem* **2002**, *3*, 1126−1133.
(47) Descours, A.; Moehle, K.; Renard, A.; Robinson, J. A. *ChemBioChem* **2002**, *3*, 318−323.

model of BIV2-TAR, the Val^2 side chain is in close contact with the RNA (not shown).

An unexpected finding is that BIV5, as the only mimetic in the library, binds not only to BIV but also to HIV-1 TAR RNA. The two additional Gly residues in BIV5, as compared to BIV2, are probably responsible for the apparent increase in conformational flexibility. NMR solution structures calculated for the major form of BIV5 in solution (data not given) showed conformations similar to those of BIV2 at the tip (residues Arg^5-Arg^8), but there appears to be more flexibility toward the center of the loop. It is possible that the dynamic behavior of BIV5, as well as the sequence, may account for its ability to bind to HIV-1 TAR RNA.

For the first time, we have been able to demonstrate strong selectivity in RNA binding by prestructuring RNA-binding peptides through the use of a β-hairpin-inducing template. The resulting structural preorganization has allowed us to collect NMR data of high quality and to observe clear structure−activity relationships. These new ligands now represent interesting leads for the development of more potent HIV TAR/Tat inhibitors, and for more detailed studies of their mechanisms of binding to both BIV and HIV-1 RNA hairpins.

Acknowledgment. We thank the Swiss National Science Foundation and the U.S. National Institute of Health NIAID for supporting this work.

Supporting Information Available: Tables of BIV2 and BIV3 ^{1}H NMR chemical shift assignments, $^3J_{HN-H\alpha}$ coupling constants, and upper-distance restraints used for structure calculations. This material is available free of charge via the Internet at http://pubs.acs.org.

JA0497680